

**Authors' response to referee comment RC1  
on manuscript  
“Development of an Automatic Linear Calibration Method for High Resolution  
Single Particle Mass Spectrometry: Improved Chemical Species Identification  
for Atmospheric Aerosols”**

We thank Referee #1 for the comments and suggestions. We have addressed every comment and made significant changes to the paper to improve the paper. Again, the referee's comments are greatly appreciated.

**Referee Comments in black bold.**

**Authors' Response in blue.**

**Changes in manuscript in Red italic.**

**Major comments**

**This paper develops an automatic linear calibration method to calibrate the mass spectra for individual particles measured by newly developed HR- SPAMS. The method improves the current accuracy of mass-to-charge ( $m/z$ ) measurement for single aerosol particles, based on the testing of laboratory-generated sea spray aerosol and atmospheric ambient aerosol. The authors provided the time series of peaks with small  $m/z$  differences and a comparison of particle classification between LR-SPAMS and HR-SPAMS. While this method may be applicable to the scientific community, there are still some limitations. The main criticism is the limited discussion of the analysis of newly generated mass spectra by the HR-SPAMS, and the lack of discussion on why only sea spray aerosols were selected. It is certainly TRUE that applying high-resolution data with enhanced mass calibration can significantly affect particle classification (identification). However, it is more important if there is new information obtained from the classification.**

Response:

We agreed that the discussions of the analysis of newly generated mass spectra by the HR-SPAMS are limited and the new information obtained from the classification is not enough in the original manuscript. In the revised manuscript, we have added the more detailed discussions of the HR-SPAMS mass spectra and illustrated why we selected sea spray aerosols as a case study, which considers the sea spray aerosol chemical compositions are relatively simple, compared to the ambient aerosol chemical compositions. The calibration method was evaluated to apply both in simple and more complicated systems. Meanwhile, based on the referee's comments, some new information, obtained from the classification, is added.

Changes in manuscript:

*Line 99-107:*

*“In this study, we report a calibration method for single particle high resolution mass spectra data. Based on the assumption that the sea spray aerosol has relatively simple chemical composition while the ambient aerosol has more complex chemical composition, the performance of the calibration method had been evaluated in detail for these two aerosol systems with different complexity. In addition, the impact of using high resolution SPAMS data on particle classification by ART-2a algorithm was assessed. An open source code specific for*

HR-SPAMS was made and we proposed the principle of this calibration method can be applied into some similar instruments, such as single particle mode Aerosol Mass Spectrometer (AMS).”

Line 273-280:

“More importantly,  $139[\text{C}_2\text{H}_3\text{O}_5\text{S}^-]$  (the theoretical  $m/z$  value: -138.97) can be clearly distinguished from other possible assignments, such as  $139[\text{C}_{11}\text{H}_7^-]$  with the  $m/z$  value of -139.55 and  $139[\text{AsO}_4^-]$  with the  $m/z$  value of -138.90. Moreover,  $153[\text{C}_3\text{H}_5\text{O}_5\text{S}^-]$  with theoretical  $m/z$  value of -152.986 can be distinguished from other possible assignments, such as  $153[\text{C}_{12}\text{H}_9^-]$  with  $m/z$  value of -153.070 and  $153[\text{Na}_2\text{Cl}_3^-]$  with  $m/z$  value of -152.883. These two important organic ion peaks have been suggested to be the characteristic ion peaks for the organosulfates in secondary organic aerosols (Surratt et al., 2010; Surratt et al., 2007).”

Line 319-347 :

“The ART-2a classification of the HR-SPAMS results (Fig.S6) show that the signal at  $23[\text{Na}^+]$  in Type 2HR was stronger than Type 1HR while the signals at  $26[\text{CN}^-]$  and  $42[\text{CNO}^-]$  were weaker in Type1 HR. Meanwhile the averaged mass spectra of the Type 2HR showed the presence of  $206[\text{Pb}^+]$ ,  $207[\text{Pb}^+]$  and  $208[\text{Pb}^+]$ , which are known to be harmful to human health (Das et al., 2018; Peng et al., 2020). Furthermore, particles of Type 2HR containing abundant secondary inorganic components like  $[\text{NO}_2^-]$ ,  $[\text{NO}_3^-]$  and  $[\text{SO}_4^-]$ , which originated from the aerosol aging processes (Dall'Osto and Harrison, 2012; Ma et al., 2016). In contrast, these two first particle types were lumped together into Type 1LR in the LR-SPAMS classification results (Fig.S5). Due to the merge of these two particle types,  $[\text{Pb}^+]$  ions were not significant. Meanwhile, Type 3,4, 5HR classification results contain strong signals at  $26[\text{CN}^-]$ ,  $42[\text{CNO}^-]$ ,  $46[\text{NO}_2^-]$ ,  $62[\text{NO}_3^-]$  and  $97[\text{HSO}_4^-]$ , suggesting that these three types were from biomass burning or residential cooking burning.  $[\text{K}^+]$  is also another feature of this type particle emission (Bi et al., 2011; Hudson et al., 2004). There were obvious relative ion intensity differences at  $26[\text{CN}^-]$ ,  $42[\text{CNO}^-]$ ,  $46[\text{NO}_2^-]$  and  $62[\text{NO}_3^-]$  among these types, which implied that these three particle types might be from different burning sources or experienced different levels of aging (Luo et al., 2020). While these three particle types were lumped together as Type 2LR. This critical information which could be potentially used to distinguish particle sources and aging processes was lost. Additionally, Type 7HR can be assigned as ECOC type, based on its strong signals at  $[\text{C}_x^+]$ ,  $[\text{C}_x\text{H}_y^+]$  and  $[\text{C}_x\text{H}_y\text{O}_z^+]$ . Particles of this type may come from the primary emission sources, and the emitted black carbon particles would also form this type particles after absorbing some low volatile organic compounds in the atmosphere (Sodeman et al., 2005).  $97[\text{HSO}_4^-]$  can be observed to have a weaker signal than  $62[\text{NO}_3^-]$  and  $46[\text{NO}_2^-]$ , which implied that the secondary reaction of  $\text{SO}_2$  as the precursor of  $\text{HSO}_4^-$  was not significant in the particle surface for ECOC type particles in this study (SULLIVAN and PRATHER, 2007). In contrast, the classification results of the LR-SPAMS were not so clear and generated less particle types. Given HR-SPAMS spectra have much more detailed chemical information about particles, we would propose that the ART-2a classification of HR-SPAMS might be more accurate.”

### Specific comments:

1. Introduction: similar instruments, such as Aerosol mass spectrometer (AMS), also have

**high-resolution versions. Is the calibration method identical to SPAMS? Inclusion of this in the introduction and discussion would be necessary for completeness.**

We agree with the referee's opinion, and decided to make an additional instruction in the introduction and conclusion for paper completeness. Our open source code of calibration method was specific for high-resolution SPAMS, while the principle of this calibration method can be applied into some similar instruments such as AMS.

Changes in manuscript:

*Line 104-107:*

*"An open source code specific for HR-SPAMS was made and we proposed the principle of this calibration method can be applied into some similar instruments, such as single particle mode Aerosol Mass Spectrometer (AMS)."*

*Line 373-376:*

*"All the automatic linear calibration method codes specific for HR-SPAMS are open access and can be found at <https://github.com/zhuxiaoqiang-fdu/zhuxiaoqiang-fdu>. And we proposed the principle of this calibration method can be adopted in other aerosol mass spectrometers."*

**2. Lines 80-85: In this section, it would be better to state the significance of why the calibration is required for each particle. While the authors noted that the ion peak position is still very susceptible to initial ion coordinate and speed, they did not provide details to show the significance.**

We agree with the referee's opinion, and added an additional statement of the reason why the calibration is required for each particle and provide the details to show the significance of the initial ion coordinate and speed.

Changes in manuscript:

*Line 85-94:*

*"Unfortunately, in spite of resolution enhancement with this new technique, ion peak position was still very sensitive to initial ion coordinate and speed. Chudinov et al., has demonstrated that the ion peak shifts of 208[Pb<sup>+</sup>] and 147[Na(NO<sub>3</sub>)<sub>2</sub><sup>-</sup>] could be varied in the range of  $\pm 10$  ns and the ion start position could be varied in the range of  $\pm 150\mu\text{m}$ . As a result, substantial peak jittering is observed when switching between mass spectra of each individual particle. This peak jittering leads to a fact that isotopic pattern identification becomes more difficult by averaged mass spectrum(Chudinov et al., 2019). Furthermore, the peak jittering is different in each single particle mass spectrum. In other words, the calibration parameter for each mass spectrum should be significantly different and calibration is required for each particle."*

**3. Line 192: "1,409 ambient particles were successfully calibrated". Why some fraction of particles cannot be calibrated? I think the discussion of such an issue in section 3.3 should be moved here to provide clear reasoning. Such an obvious deficiency should also be stated in the abstract or conclusion.**

We agree with the referee's opinion that it's an obvious deficiency. This is mainly due to the reason that we set the threshold of absolute ion intensity 15 a.u for marker ions in the

ambient aerosols and 8 a.u in the sea spray aerosols. And a particle was discarded from the spectrum database if it did not have enough reference ions ( the minimum number of reference ions was set to be 5) in either positive or negative mass spectrum. And now we have made a clear reasoning in the section 3.2 and also stated in the conclusion.

Changes in manuscript:

*Line 210-213:*

*“And 4,624 sea spray particles and 1,409 ambient particles were successfully calibrated. As some fraction of particles had been filtered because their mass spectrum did not have 5 or more reference peaks to conduct the calibrations. To mitigate this problem, we proposed some adjustments in the next section.”*

*Line 370-373:*

*“There is a deficiency of this HR-SPAMS calibration method, which has been showed that some fraction of particles cannot be calibrated due to the presence of weak signals of the marker ions. It can be mitigated by applying some additional marker ions.”*

**4. What is the matrix size produced by the HR-SPAMS? Is there a limit for the ART-2a to classify the matrix of particle mass spectra? Such information should be included.**

As there is 25,000 bins in either positive or negative single mass spectrum and we handled about 1,400 particles in this study. The matrix size is about  $25,000 \times 2 \times 1400 = 7e7$ . There was no absolute limit for ART-2a as long as the database was not extremely large, like the experiment data lasting for several months. And we have made the following additional statement to include this necessary information in our revised manuscript.

Changes in manuscript:

*Line 305-306 :*

*“The previous ambient aerosol SPAMS dataset (1,400 particles) was used for the matrix size of the ART-2a is around  $7 \times 10^7$ .”*

**5. Section 4.4: What kind of new information is provided when new matrix is included in the classification? I think it would be interesting if there is new information after the classification of newly calibrated mass spectra.**

It is the same comment as the referee's major comments. We agree with the referee's comment that the discussions of our new classification results are not quite sufficient in our original manuscripts. And now we have made a more comprehensive discussions, as we responses to the referee's major comments above.

**6. Some peak ions should be added to Fig S5 and Fig S6 for clearance.**

We have added the necessary peak ions in the Fig S5 and Fig S6 for clearance in our revised supplement.

Changes in supplementary material:

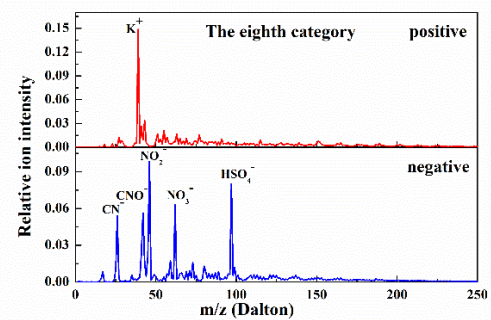
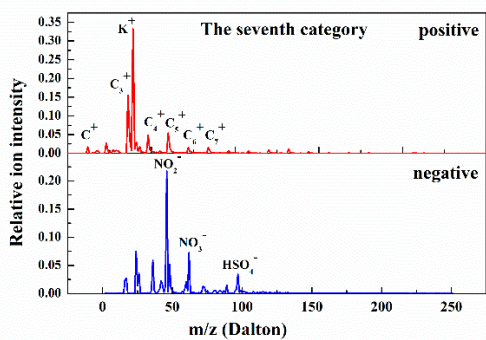
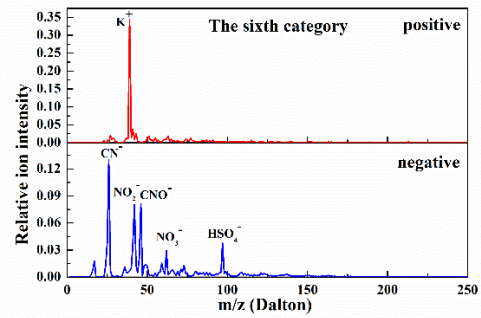
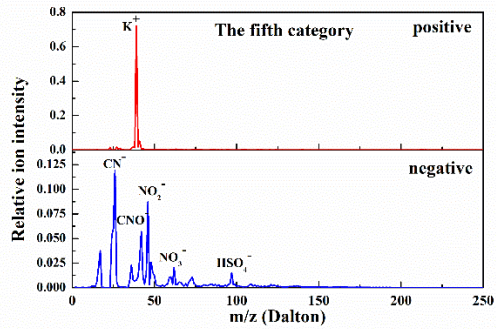
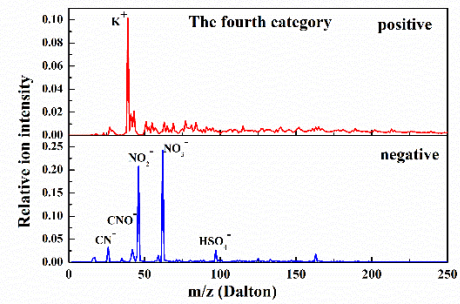
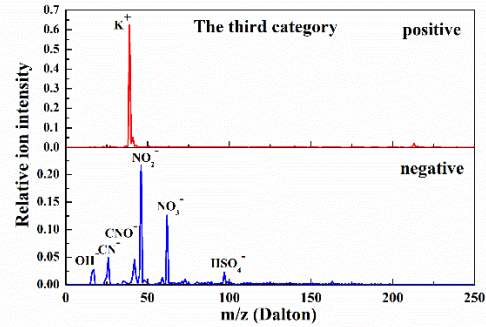
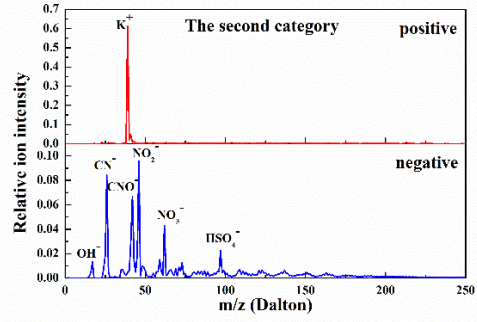
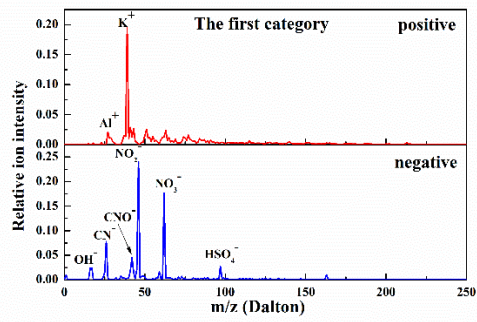


Figure.S5 Classification results of the LR-SPAMS by ART-2a

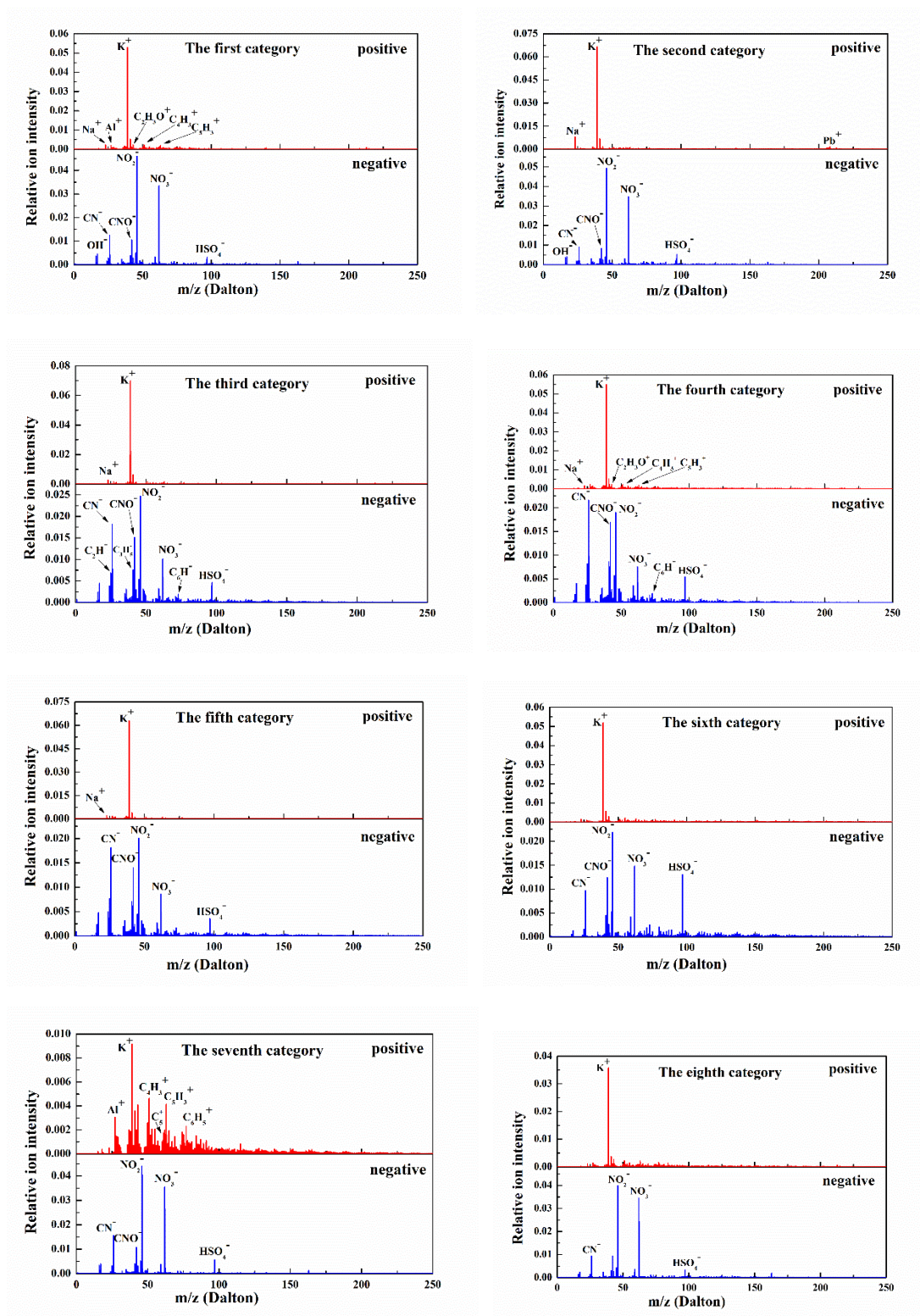


Figure.S6 Classification results of the HR-SPAMS by ART-2a

7. Conclusion: It would be better to include some atmospheric implications for the identification of additional peaks, in particular, organic peaks. Currently, the authors showed that more particle types can be obtained, but it might not be meaningful enough for the scientific community.

We agree with the referee's comments and here is the revision:

Changes in manuscript:

*Line 358-370:*

*“With this method, HR-SPAMS can also determine the time series of organic and inorganic peaks, whose  $m/z$  are very close to each other (e.g.  $41K^+$  with the theoretical  $m/z$  value at 40.96182 and  $C_3H_5^+$  with the theoretical  $m/z$  value at 41.03913). Important organic ion peaks, such as tracer peaks for secondary organic matter like  $139[C_2H_3O_5S^-]$  and  $153[C_3H_5O_5S^-]$ , can be identified. More importantly, our ART-2a classification from HR-SPAMS dataset clearly showed a particle type containing heavy metals like  $Pb^+$ , which was obviously ignored in the ART-2a classification from the LR-SPAMS dataset. More particle types were generated by the ART-2a classification of HR-SPAMS data compared to that of LR-SPAMS data, as the original biomass burning particle type can be divided into three more detailed types based on the different signals of  $26[CN^+]$ ,  $42[CNO^+]$ ,  $46[NO_2^+]$  and other organic species like  $C_xH_y$  and  $C_xH_yO_z$ , implying different aerosol aging processes or burning conditions. Such detailed information may be critical to study the aging processes and source appointment of atmospheric aerosols.”*

## **8. Grammar check**

**Line 70: LDI?**

**Line 77: “A SPAMS”**

**Line 99: “accessed”**

We have made correction to the grammar issues.

Changes in manuscript:

*Line 71-72:*

*“However, SPAMS with laser desorption/ ionization (LDI) method has several serious limitations (Manuel et al., 2006; Wenzel et al., 2003).”*

*Line 79:*

*“A higher mass resolution version of the SPAMS with better  $m/z$  accuracy is needed.”*

*Line 103-104:*

*“In addition, the impact of using high resolution SPAMS data on particle classification by ART-2a algorithm was assessed.”*

**Authors' response to referee comment RC2  
on manuscript  
“Development of an Automatic Linear Calibration Method for High Resolution  
Single Particle Mass Spectrometry: Improved Chemical Species Identification  
for Atmospheric Aerosols”**

We thank Referee #2 for the comments and suggestions. We have addressed every comment and made significant changes to improve the paper. Again, the referee's comments are greatly appreciated.

**Referee Comments in black bold.**

Authors' Response in blue.

Changes in manuscript in Red italic.

**Major comments**

This study reports the development of an automatic linear calibration method for analyzing mass spectral data acquired with single particle mass spectrometers with mass resolution of  $\sim 2000$ . The paper also shows the successful application of this method to analyzing lab generated sea spray particles and some ambient aerosols. This work is important given the broad application of single particle mass spectrometry in atmospheric studies and aerosol research and improvement of the chemical resolution of this technique is important. The scope of the work fits well within AMT and the manuscript is generally well written. I recommend acceptance for publication after following comments are addressed.

Response:

We are grateful for the comments given by the referee and hope our new automatic linear calibration method can be applied into more versions of aerosol mass spectrometry for atmospheric studies. Also we have addressed all the comments in the following paragraphs.

**Specific comments :**

**1. Line 119,change to “dried by”**

We have made correction to that.

Changes in manuscript:

*Line 135-136:*

*“The ambient particles were dried by a diffusional dryer before being sampled by the HR-SPAMS.”*

**2. Fig. S2, the caption for this figure needs to be rewritten to better present the information content.**

We have rewritten the caption of the Fig.S2 to better present the information content.

Changes in supplementary material:

*“Fig.S2 partial enlarged detail in the sing particle mass spectra for the*



*explanation of the m/z bin value”*

Changes in manuscript:

*Line 141-144:*

*“Noticeably, due to the technical limitation of data acquisition, the whole HR-SPAMS spectrum is not continuous but divided by a large number of m/z bins, which are described in Fig.S2(a partial enlarged detail in the single particle mass spectra) and can be viewed as the probability density histogram of the m/z.”*

**3. Line 171, what does a.u. stand for? How were the thresholds selected?**

a.u. stands for the arbitrary unit, which is used widely in the averaged aerosol mass spectra for ion intensity. The absolute ion intensity threshold adopted in the YAADA (Yet Another ATOFMS DATA Analyzer, [www.yaada.org](http://www.yaada.org)) for SPAMS is 5 a.u., so the thresholds we used (15 a.u. for ambient aerosol and 8 a.u. for sea spray aerosol) can be considered reasonable just in case of the interfering signals in the aerosol mass spectra.

**4. The description on Step 3 given in the paragraph on pages 6 and 7 is a bit hard to follow. How exactly is the calibration conducted? Are the measured m/z bins determined from the “traditional method” mentioned in Step 0? What exactly is the “traditional method” involved? How many bins are selected for each m/z?**

(1)The detailed statement of the Step 3 is that: First, we will get the measured m/z bins determined from the “traditional method”, just as described in the Step 0. And these bins were not sufficiently accurate. Then, we picked up some reference ions to make a linear regression between the two set of variables (measured vs. theoretic reference ion m/z bin values). The obtained calibration parameters (a slope and an intersect) from linear regression were used to calibrate every bin value for this mass spectrum. However, the m/z bin values are fixed numbers (they are not continuous). So we had to assign the calibrated m/z value to its closest m/z bin value. Finally, the correct aerosol mass spectra can be acquired. We had made some revisions to make it easier to read in the Step3;

(2)The measured m/z bin values were determined from the “traditional method” mentioned in the Step 0;

(3)The “traditional method” was more like a coarsely-calibrated method, which usually selected a few particles with distinct ion patterns. Fig3 and Table S1&S2 had reported there were around five of larger bin numbers offset for the ionized species. What’s more important is that every particle mass spectra were different from each other and needed its own calibration parameters. So the “traditional method” is not enough for the SPAMS data processing.

(4)One specific bin was selected for each m/z as shown in the Fig.S2

Changes in manuscript:

*Line 193-195:*

*“The measured m/z bin values of the reference ions mentioned in the Step0 were calibrated based on their theoretic (or true) m/z bin values.”*

*Line 197-199:*

*“Then we used these parameters to make the calibration for every bin value in this mass spectra. Finally, the m/z of the whole spectrum had been corrected.”*

**5. Give units for “measurement m/z” and “theoretical m/z” on the axis labels in all the Figures presented in this paper.**

The unit is Dalton. We have updated all m/z axis labels in in the revised paper.

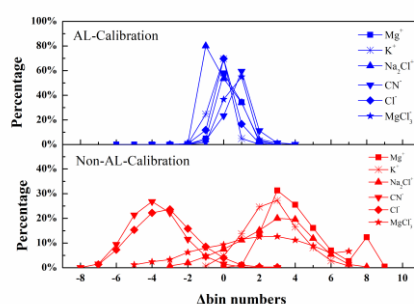
**6. Figure 3, the symbols are hard to differentiate, consider to revise. The spectra a and b look identical, are they really represent sea spray aerosol and ambient aerosol respectively?**

Thanks for pointing this out. It was a mistake and has been corrected now. We have also separated the figure into 2 panels to make them easier to differentiate.

Changes in manuscript:

*Line 548-553:*

*“a.*



*b.*

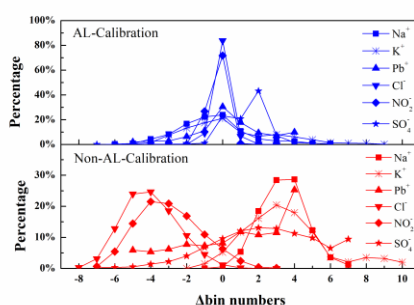


*Figure 3. Probability distributions of the marker peak locations before and after Automatic Linear Calibration (AL-Cal) for (a) sea spray aerosol and (b) ambient aerosol “*

**7. Figure 4, what is “error limits”? How was is calculated?**

The “error limit” is the delta bin number which is concluded from the Table S1&S2 and Fig.3,

representing the accepted error range (around 3 bin numbers) after the calibration for a m/z bin value.

Changes in manuscript:

*Line 252-254:*

*“Figure 4 reports the average positive and negative mass spectra for the laboratory generated sea spray aerosols and the error limits mean the concluded accepted error range.”*

**7. Line 250, change to “Ca<sup>2+</sup>”**

Actually the ion fragment generated from the SPAMS can only carry one charge, so the Ca<sup>+</sup> is reasonable.

**9. Line 266, define “LR-SPAMS”?**

We have give a definition for that.

Changes in manuscript:

*Line 295-297:*

*“In contrast, it is impossible for a low resolution (LR)-SPAMS to provide such detailed time variation measurement of these peaks.”*

1       **Development of an Automatic Linear Calibration Method for High**  
2       **Resolution Single Particle Mass Spectrometry: Improved Chemical**  
3       **Species Identification for Atmospheric Aerosols**

4  
5  
6       **Authors:** Shengqiang Zhu<sup>1</sup>, Lei Li<sup>2</sup>, Shurong Wang<sup>1</sup>, Mei Li<sup>2</sup>, Yaxi Liu<sup>1</sup>, Xiaohui  
7       Lu<sup>1</sup>, Hong Chen<sup>1</sup>, Lin Wang<sup>1,3</sup>, Jianmin Chen<sup>1,3</sup>, Zhou Zhen<sup>2</sup>, Xin Yang<sup>\*1,3,4</sup> and Xiaofei  
8       Wang<sup>\*1,3</sup>

9  
10       <sup>1</sup>*Shanghai Key Laboratory of Atmospheric Particle Pollution and Prevention,*  
11       *Department of Environmental Science and Engineering, Fudan University, Shanghai*  
12       *200433, China*

13       <sup>2</sup>*Institute of Mass Spectrometer and Atmospheric Environment, Jinan University,*  
14       *Guangzhou, 510632, China*

15       <sup>3</sup>*Shanghai Institute of Pollution Control and Ecological Security, Shanghai 200092,*  
16       *China*

17       <sup>4</sup>*School of Environmental Science and Engineering, Southern University of Science*  
18       *and Technology, Shenzhen 518055, China*

19  
20       **Atmospheric Measurement Techniques**

21  
22       June 3<sup>rd</sup>, 2020

23  
24  
25       \*To whom correspondence should be addressed.

26  
27       Correspondence to:

28       Xiaofei Wang

29       Email: [xiaofeiwang@fudan.edu.cn](mailto:xiaofeiwang@fudan.edu.cn) Tel: +86-21-31242526

30       Xin Yang

31       Email: [yangxin@fudan.edu.cn](mailto:yangxin@fudan.edu.cn) Tel: +86-21-31245272

32

33 **Abstract**

34

35 The mass resolution of laser desorption ionization (LDI) single particle aerosol mass  
36 spectrometry (SPAMS) is usually low ( $\sim 500$ ), which has been greatly improved by recent  
37 development of delayed ion extraction technique. However, due to large fluctuations  
38 among LDI processes during each laser shot, accurate calibration of mass-to-charge ratio  
39 for high resolution SPAMS spectra is challenging. Here we developed an automatic linear  
40 calibration method to improve the accuracy of mass-to-charge ( $m/z$ ) measurement for  
41 single atmospheric aerosol particles. Laboratory generated sea spray aerosol and  
42 atmospheric ambient aerosol were tested. After the calibration, the fluctuation ranges of  
43 the reference ions (e.g.  $\text{Pb}^+$  and  $\text{SO}_4^+$ )  $m/z$  reaches  $\pm 0.018$  for sea spray aerosol and  $\pm$   
44  $0.024$  for ambient aerosol in average mass spectra. With such  $m/z$  accuracy, the HR-  
45 SPAMS spectra of sea spray aerosol can easily identify elemental compositions of organic  
46 peaks, such as  $\text{C}_x$ ,  $\text{C}_x\text{H}_y$  and  $\text{C}_x\text{H}_y\text{O}_z$ . While the chemical compositions of ambient aerosols  
47 are more complicated,  $\text{C}_x\text{H}_y$ ,  $\text{C}_x\text{H}_y\text{O}_z$  and CNO peaks can also be identified based on their  
48 accurate mass. With the improved resolution, the time series of peaks with small  $m/z$   
49 differences can be separated and measured. In addition, it is also found that applying high  
50 resolution data with enhanced mass calibration can significantly affect particle  
51 classification (identification) using the ART-2a algorithm, which classify particles based on  
52 similarities among single particle mass spectra.

53

54

## 55 1. Introduction

56

57 Atmospheric aerosols can significantly impact radiative forcing, cloud formation and  
58 human health(Ackerman et al., 2004; Zhang and Kin-Fai, 2012). They originate from  
59 various sources and undergo many atmospheric aging processes, resulting in an extremely  
60 complicated mixture of particles with a large range of sizes and chemical compositions.  
61 This mixture is usually referred as “mixing state”. Measurement of aerosol mixing state  
62 requires single particle characterization techniques. Utilizing laser ablation/ionization of  
63 single aerosol particle, Single Particle Aerosol Mass Spectrometer (SPAMS) has been  
64 widely used to measure chemical compositions, sizes and refractory index of aerosols in  
65 real-time(Moffet and Prather, 2009; Murphy, 2010; Sullivan and Prather, 2005). Based on  
66 this technique, ART-2a and other algorithms had been developed to classify the ambient  
67 particles based on their mass spectra and identify their sources (Reinard et al., 2007;  
68 Zelenyuk and Imre, 2009).

69

70

71 **However, SPAMS with laser desorption/ ionization (LDI) method has several serious**  
72 **limitations** (Manuel et al., 2006; Wenzel et al., 2003). A major issue is that the mass  
73 resolution of the SPAMS is relatively low (~500) and the accuracy of m/z (mass to charge  
74 ratio) is usually at integer level, resulting in uncertainties about the identification of  
75 chemical species (Nash et al., 2006; Pratt and Prather, 2012; Qin et al., 2006). Due to the  
76 low mass resolution, many organic and inorganic peaks cannot be separated, such as  $K^+$   
77  $/C_3H_3^+$  from the m/z peak of 39,  $Al^+ C_2H_3^+$  from the m/z peak of 27 and  $CN^- /C_2H_2^-$  from  
78 the m/z peak of -26 (Li et al., 2018). To better identify these particulate chemical species,  
79 **A higher mass resolution version of the SPAMS with better m/z accuracy is needed.**

80

81

82 Recently, Li et al., significantly increased SPAMS’s mass resolution to ~2000 by applying  
83 delayed ion extraction technique, which combined a standard rectangular extraction pulse  
84 with an exponential pulse (Li et al., 2018). This new SPAMS is called high resolution (HR)-  
85 SPAMS. **Unfortunately, in spite of resolution enhancement with this new technique, ion**

86 peak position was still very sensitive to initial ion coordinate and speed. Chudinov et al.,  
87 has demonstrated that the ion peak shifts of  $208[\text{Pb}^+]$  and  $147[\text{Na}(\text{NO}_3)_2^-]$  could be varied  
88 in the range of  $\pm 10$  ns and the ion start position could be varied in the range of  $\pm 150\mu\text{m}$ .  
89 As a result, substantial peak jittering is observed when switching between mass spectra of  
90 each individual particle. This peak jittering leads to a fact that isotopic pattern identification  
91 becomes more difficult by averaged mass spectrum (Chudinov et al., 2019). Furthermore,  
92 the peak jittering is different in each single particle mass spectrum. In other words, the  
93 calibration parameter for each mass spectrum should be significantly different and  
94 calibration is required for each particle. Therefore, in order to get accurate m/z, Chudinov  
95 et al. used several peaks with known m/z to calibrate every SPAMS spectrum for  $\text{Pb}(\text{NO}_3)_2$   
96 and NaI particles produced from an atomizer.

97  
98  
99 In this study, we report a calibration method for single particle high resolution mass spectra  
100 data. Based on the assumption that the sea spray aerosol has relatively simple chemical  
101 composition while the ambient aerosol has more complex chemical composition, the  
102 performance of the calibration method had been evaluated in detail for these two aerosol  
103 systems with different complexity. In addition, the impact of using high resolution SPAMS  
104 data on particle classification by ART-2a algorithm was assessed. An open source code  
105 specific for HR-SPAMS was made and we proposed the principle of this calibration method  
106 can be applied into some similar instruments, such as single particle mode Aerosol Mass  
107 Spectrometer (AMS).

108  
109  
110 However, atmospheric particles are extremely complicated with a wide range of chemical  
111 compositions and sizes (Zhang et al., 2013), which brings much greater challenge to  
112 properly calibrating each SPAMS mass spectra and obtaining accurate m/z measurement.  
113 We need to develop a new MS calibration method for atmospheric aerosols and evaluate  
114 its performance comprehensively.

115  
116

## 117 **2. Experimental Section**

### 118 **2.1 High Resolution Single Particle Aerosol Mass Spectrometer (HR-SPAMS)**

119 The detailed description of HR-SPAMS (Hexin Analytical Instrument Co., Ltd., China) can  
120 be found elsewhere(Li et al., 2018). Briefly, a HR-SPAMS consists of an aerodynamic lens  
121 as its particle inlet, two laser beams system for particle sizing, a UV laser for LDI and a  
122 bipolar time-of-flight mass analyzer for the detection of positive and negative ions. Positive  
123 and negative ions are detected by two z-shape bipolar TOF reflectron mass analyzers. The  
124 size detection range of HR-SPAMS is 200-2000 nm. As introduced before, this HR-SPAMS  
125 used delayed ion extraction technique to enhance its mass resolution.

126

### 127 **2.2 Laboratory generated sea spray aerosol**

128 Sea spray aerosol was produced by water jet method. In a sea spray aerosol production  
129 tank, a seawater jet was hitting seawater surface and producing bubbles, which would rise  
130 to the surface and burst. Bubble bursting process produces sea spray aerosols. Seawater  
131 was collected at Fengxian, Shanghai (30°92'N and 121°47'E) on March 30<sup>st</sup> (Fig.S1).

132

### 133 **2.3 Ambient aerosol sampling**

134 Ambient aerosol sampling was conducted at Fudan university, Shanghai (31°20'N and  
135 121°30'E) on May 29<sup>th</sup> 2019 (Fig.S1). **The ambient particles were dried by a diffusional  
136 dryer before being sampled by the HR-SPAMS.**

137

## 138 **3. Development of Calibration Methods**

### 139 **3.1 Automatic linear calibration method**

140 To improve the accuracy of m/z for HR-SPAMS spectra, an automatic linear calibration  
141 method has been developed. **Noticeably, due to the technical limitation of data acquisition,  
142 the whole HR-SPAMS spectrum is not continuous but divided by a large number of m/z  
143 bins, which are described in Fig.S2(a partial enlarged detail in the single particle mass  
144 spectra) and can be viewed as the probability density histogram of the m/z.** Here we denote  
145 “m/z bin value” as the median m/z value of each bin.

146

147 The linear calibration method is described as the following steps:



148

149 Step 0: The SPAMS data was coarsely-calibrated by the traditional method, which usually  
150 selected a few particles with distinct ion patterns, i.e. the molecular composition of some  
151 distinct peaks in the mass spectra can be easily identified. Then, the time of flight of these  
152 peaks and the true m/z of the corresponding ions were used to calculate a set of calibration  
153 parameters for positive and negative spectra. The parameters were finally applied to the  
154 whole mass spectra dataset, and coarsely-calibrated was completed.

155

156 Step 1: a pool of ion peaks in the single particle mass spectra were selected as the potential  
157 m/z calibration reference ions. The selection criteria are (1) these peaks should be present  
158 in most of the spectra; (2) the identification of these ion peaks should not be significantly  
159 affected by other adjacent peaks. For example, 27[Al]<sup>+</sup> was not selected, as its adjacent  
160 peak 27[C<sub>2</sub>H<sub>3</sub>] may affect the peak shape and identification of 27[Al] .

161

162 According to the previous research, possible peak assignments for the m/z of reference ions  
163 for sea spray aerosol and ambient aerosol were listed on Table 1(Bertram et al., 2018;  
164 Collins et al., 2014; Tsunogai et al., 1972; Wang et al., 2016; Wang et al., 2019). For sea  
165 spray aerosol, according to several studies (Bertram et al., 2018; Collins et al., 2014;  
166 Tsunogai et al., 1972), the reference ions with m/z 23 24 39 -35 -37 were 23[Na]<sup>+</sup> 24[Mg]<sup>+</sup>  
167 39[K]<sup>+</sup> -35[Cl]<sup>-</sup> and -37[Cl]<sup>-</sup> respectively. And Collins et al. shows that the reference ions  
168 with m/z 81, 83, -26, -42, -58, -129, and -131 were 81[Na<sub>2</sub>Cl] , 83[Na<sub>2</sub>Cl] , -26[CN] , -  
169 42[CNO]<sup>-</sup>, -58[NaCl]<sup>-</sup>, -129[MgCl<sub>3</sub>]<sup>-</sup>, and -131[MgCl<sub>3</sub>]<sup>-</sup>, respectively (Collins et al., 2014).  
170 Due to the fact that Na, Mg and K were abundant in sea spray aerosol, the reference ions  
171 with m/z 113 and 115 should be 113[K<sub>2</sub>Cl]<sup>+</sup> and 115[K<sub>2</sub>Cl]<sup>+</sup>. Thus, in this study, we select  
172 23[Na]<sup>+</sup>, 24[Mg]<sup>+</sup>, 39[K]<sup>+</sup>, 81[Na<sub>2</sub>Cl]<sup>+</sup>, 83[Na<sub>2</sub>Cl]<sup>+</sup>, 113[K<sub>2</sub>Cl]<sup>+</sup>, 115[K<sub>2</sub>Cl]<sup>+</sup>, -35[Cl]<sup>-</sup>, -  
173 37[Cl]<sup>-</sup>, -26[CN]<sup>-</sup>, -42[CNO]<sup>-</sup>, -129[MgCl<sub>3</sub>]<sup>-</sup>, -131[MgCl<sub>3</sub>]<sup>-</sup>, -58[NaCl]<sup>-</sup> as the potential  
174 reference ions for sea spray aerosols.

175

176 For the ambient aerosol, according to the previous ambient SPAMS measurements(Wang  
177 et al., 2016; Wang et al., 2019), the reference ions with m/z 12, 23, 36, 39, 56, 207, 208,  
178 and 209 were assigned to 12[C]<sup>+</sup>, 23[Na]<sup>+</sup>, 36[C<sub>3</sub>]<sup>+</sup>, 39[K]<sup>+</sup>, 56[Fe]<sup>+</sup>, 207[Pb]<sup>+</sup>, 208[Pb]<sup>+</sup>

179 and  $209[\text{Pb}]^+$ , the reference ions with  $m/z$  -26, -35, -46, -62, -96, and -97 were assigned to  
180  $-26[\text{CN}]^-$ ,  $-35[\text{Cl}]^-$ ,  $-46[\text{CNO}]^-$ ,  $-62[\text{NO}_2]^-$ ,  $-96[\text{SO}_4]^-$  and  $-97[\text{HSO}_4]^-$  respectively. So in  
181 this study, we select the  $12[\text{C}]^+$ ,  $23[\text{Na}]^+$ ,  $39[\text{K}]^+$ ,  $36[\text{C}_3]^+$ ,  $56[\text{Fe}]^+$ ,  $208[\text{Pb}]^+$ ,  $206[\text{Pb}]^+$ ,  
182  $207[\text{Pb}]^+$ ,  $-62[\text{NO}_3]^-$ ,  $-26[\text{CN}]^-$ ,  $-35[\text{Cl}]^-$ ,  $-96[\text{SO}_4]^-$ ,  $-46[\text{NO}_2]^-$ ,  $-97[\text{HSO}_4]^-$  as the  
183 potential reference ions for ambient aerosols.

184

185 Step 2: a set of reference ions was chosen from the potential reference ion pool for each  
186 spectrum. The selection was based on the absolute ion intensity of the reference ions in this  
187 spectrum. They must be greater than a threshold, e.g. we set 15 a.u. for ambient aerosol  
188 and 8 a.u. for sea spray aerosol, respectively. A particle was discarded from the spectra  
189 database if it did not have enough reference ions (the minimum number of reference ions  
190 was set to be 5) in either positive or negative mass spectrum.

191

192 Step 3: the reference ions were used to calibrate  $m/z$  for mass spectra of each particle. As  
193 introduced before, a HR-SPAMS spectrum consists of a number of bins. **The measured  $m/z$   
194 bin values of the reference ions mentioned in the Step0 were calibrated based on their  
195 theoretic (or true)  $m/z$  bin values.** A linear regression between the two set of variables  
196 (measured vs. theoretic  $m/z$  bin values) was conducted, and two calibration parameters (a  
197 slope and an intersect) can be obtained. **Then we used these parameters to make the  
198 calibration for every bin value in this mass spectra. Finally, the  $m/z$  of the whole spectrum  
199 had been corrected.** Thus, we assigned a  $m/z$  bin value to each corrected  $m/z$  based on  
200 proximity principle. Finally, mass spectra with well calibrated bin value can be obtained  
201 for each single particle.

202

203 A GUI program for this automatic linear calibration method had been developed for the  
204 sake of easy use (Fig. 1). The MATLAB codes for this GUI and the automatic linear  
205 calibration method are open access and available at [https://github.com/zhuxiaoqiang-  
206 fdu/zhuxiaoqiang-fdu](https://github.com/zhuxiaoqiang-fdu/zhuxiaoqiang-fdu).

207

### 208 **3.2 Evaluation of the calibration method**

209 In this study, a total of 5,130 sea spray aerosol particles and 5,007 ambient aerosol particles

210 were analyzed. And 4,624 sea spray particles and 1,409 ambient particles were successfully  
211 calibrated. As some fraction of particles had been filtered because their mass spectrum did  
212 not have 5 or more reference peaks to conduct the calibrations. To mitigate this problem,  
213 we proposed some adjustments in the next section. Figure 2 shows that the calibration  
214 curves for a random selected sea spray aerosol particle and ambient aerosol particle. The  
215 adj-R<sup>2</sup> coefficients of both calibration curves are equal to ~1, demonstrating that this  
216 calibration method is effective and accurate. All the slopes and intercepts of the linear  
217 calibration can be found in the Fig.S3 and Fig.S4. In addition, Figure 3a and 3b report a  
218 comparison of m/z distributions of reference ions between before and after automatic linear  
219 calibration. The results show that the fluctuations of the reference ions m/z were  
220 significantly reduced after automatic linear calibration. The average m/z deviation of the  
221 reference ions was reduced from ~0.04 to ~0.001 for sea spray aerosol, and from ~0.035  
222 to ~0.006 for ambient aerosol, respectively.

223

### 224 **3.3 Automatic linear calibration method with a larger reference ion pool**

225 It is important to note that a large number of ambient particles were filtered because their  
226 spectra did not have 5 or more reference peaks to conduct calibrations. Especially, only  
227 ~29.0% of total ambient particles had sufficient number of reference ions in their positive  
228 spectra. To solve this problem, extra reference ions, including 67[VO]<sup>+</sup>, 67[C<sub>5</sub>H<sub>7</sub>]<sup>+</sup>,  
229 89[C<sub>7</sub>H<sub>5</sub>]<sup>+</sup>, 89[Na<sub>2</sub>BO<sub>2</sub>]<sup>+</sup>, 102[C<sub>8</sub>H<sub>6</sub>]<sup>+</sup>, 102[CaNO<sub>3</sub>]<sup>+</sup>, were added into the original positive  
230 reference ion pool. Obviously, these ions share the same integer m/z value with other ions.  
231 We needed to identify them using additional information other than their integer m/z values.

232

233 The specific reference ions was determined by their coarsely-calibrated m/z. Table S2  
234 shows that the m/z deviation ranges of the reference positive ambient ions in coarsely-  
235 calibrated spectra before automatic linear calibration were around 0.011~0.048, while the  
236 m/z differences between 67[VO]<sup>+</sup> and 67[C<sub>5</sub>H<sub>7</sub>]<sup>+</sup>, 89[C<sub>7</sub>H<sub>5</sub>]<sup>+</sup> and 89[Na<sub>2</sub>BO<sub>2</sub>]<sup>+</sup>, 102[C<sub>8</sub>H<sub>6</sub>]<sup>+</sup>  
237 and 102[CaNO<sub>3</sub>]<sup>+</sup> were 0.1213, 0.0622, and 0.083, respectively, which were larger than the  
238 m/z deviations of these reference ions in coarsely-calibrated spectra. Therefore, the  
239 coarsely-calibrated spectra can be used to determine these specific reference ions. With  
240 these additional potential reference ions, a total of 2490 ambient particles were calibrated,

241 much more than the previous analysis (1,409 ambient particles). The deviations from  
242 theoretical  $m/z$  for applying this expanded ion pool are summarized in Table S3. The  
243 average  $m/z$  deviation of the reference ions is  $\sim 0.0068$ .

244

## 245 **4. Application to atmospheric aerosols measurement**

### 246 **4.1 HR-SPAMS measurement of sea spray aerosol**

247 SPAMS data usually contains a large number of individual mass spectra. It is impossible  
248 to manually analyze every spectrum from a large dataset. Averaging a number of mass  
249 spectra is often preferred. However, to obtain averaged high-resolution spectrum, each  
250 spectrum must be well calibrated. Therefore, it would be very interesting to see what new  
251 information can be obtained from HR-SPAMS measurement of aerosols with the automatic  
252 calibration method. **Figure 4 reports the average positive and negative mass spectra for the**  
253 **laboratory generated sea spray aerosols and the error limits mean the concluded accepted**  
254 **error range.** Similar to the low-resolution sea spray aerosol mass spectra, they contain  
255 major peaks of  $\text{Na}^+$ ,  $\text{Mg}^+$ ,  $\text{K}^+$ ,  $\text{Na}_2\text{Cl}^+$ ,  $\text{CN}^-$ ,  $\text{Cl}^-$ ,  $\text{CNO}^-$ ,  $\text{NaCl}^-$ ,  $\text{NaCl}_2^-$  and  $\text{MgCl}_3^-$ , as well  
256 as many smaller peaks, such as  $\text{Ca}^+$ ,  $\text{SiO}_2^-/\text{SiO}_3^-$ , and  $\text{KCl}_2^-$ . With the improved  $m/z$   
257 measurement, many peaks, which cannot be determined by integer resolution mass spectra,  
258 now can be clearly identified (Table 2). For example, the ion with  $m/z$  at 27.0267 is  $\text{C}_2\text{H}_3^+$   
259 rather than  $\text{Al}^+$ . The ion with  $m/z$  at 76.9336 is  $\text{CaCl}^+$  rather than  $\text{C}_6\text{H}_5^+$ . And some sulfur  
260 containing organic ions, such as  $\text{CS}^+$ , can be determined. Surprisingly, we can identify the  
261 presence of  $\text{HCO}_2^-$  and  $\text{CaCO}_3^-$ , demonstrating that carbon hydrates are contained in sea  
262 spray aerosols.

263

### 264 **4.2 HR-SPAMS measurement of atmospheric aerosol**

265 Laboratory generated sea spray aerosol can be viewed as a relatively simple aerosol system,  
266 while the chemical compositions of ambient aerosols are much more complicated. Figure  
267 5 shows the averaged HR-SPAMS mass spectra of the ambient aerosols sampled at Fudan  
268 University Jiangwan Campus on May 29<sup>th</sup>, 2019. With the improved  $m/z$  measurement,  
269 many organic ions, such as  $\text{C}_x$ ,  $\text{C}_x\text{H}_y$ , and  $\text{C}_x\text{H}_y\text{O}_z$  can be directly identified (Table 3). Also,  
270 we can separate the organic and inorganic species more directly with the high mass  
271 resolution. For instance,  $\text{C}_6\text{H}_8^+$  can be clearly distinguished from possible interference of

272  $\text{Ca}_2^-$ ,  $\text{TiO}_2^+$  and  $\text{NaKO}^+$ .  $\text{C}_{10}\text{H}^-$  can also be identified from possible assignment of  $\text{NaSO}_4^-$   
273 etc. More importantly,  $139[\text{C}_2\text{H}_3\text{O}_5\text{S}^-]$  (the theoretical m/z value: -138.97) can be clearly  
274 distinguished from other possible assignments, such as  $139[\text{C}_{11}\text{H}_7^-]$  with the m/z value of  
275 -139.55 and  $139[\text{AsO}_4^-]$  with the m/z value of -138.90. Moreover,  $153[\text{C}_3\text{H}_5\text{O}_5\text{S}^-]$  with  
276 theoretical m/z value of -152.986 can be distinguished from other possible assignments,  
277 such as  $153[\text{C}_{12}\text{H}_9^-]$  with m/z value of -153.070 and  $153[\text{Na}_2\text{Cl}_3^-]$  with m/z value of -  
278 152.883. These two important organic ion peaks have been suggested to be the  
279 characteristic ion peaks for the organosulfates in secondary organic aerosols (Surratt et al.,  
280 2010; Surratt et al., 2007).

281

282

### 283 4.3 Time variation of HR-SPAMS measurement

284 With the high mass resolution of HR-SPAMS and enhanced m/z calibration, we were able  
285 to obtain an average mass spectrum from many particles. The accurate m/z values in the  
286 average mass spectrum can be used to separate peaks with close m/z and track their  
287 intensity variations. Here we conducted a time variation measurement for ambient aerosol  
288 from 11:00 on May 29<sup>th</sup> to 11:00 on May 30<sup>th</sup>2019. We selected first 500 particles collected  
289 by SPAMS during every hour for elemental analysis. Figure 6 shows that the peak at m/z  
290 41 has a bimodal structure, whose m/z were at  $40.9546 \pm 0.0105$  and  $41.0194 \pm 0.0105$ ,  
291 respectively. Thus the peak with the smaller m/z is an isotope of  $\text{K}^+$  (theoretical m/z value  
292 of  $^{41}\text{K}^+ = 40.96182$ , theoretical m/z bin value of  $^{41}\text{K}^+ = 40.9667$ ; this peak also follows the  
293 isotopic pattern of K) and the other peak should be  $\text{C}_3\text{H}_5^+$  (theoretical m/z value 41.03913,  
294 theoretical m/z bin value 41.03). Figure 6 shows that HR-SPAMS was able to separately  
295 measure the time series of these two peaks with a small m/z difference. In contrast, it is  
296 impossible for a low resolution (LR)-SPAMS to provide such detailed time variation  
297 measurement of these peaks.

298

### 299 4.4 Particle classification by ART-2a

300 Adaptive resonance theory neural network (ART-2a) is a widely-used method to classify  
301 particles based on the similarity among their mass spectra (Song et al., 1999). Here we  
302 make a comparison of ART-2a classification between the HR-SPAMS data and traditional

303 low resolution (LR)-SPAMS data. Particles with the positive and negative spectra were  
304 analyzed by ART-2a with a learning rate of 0.05, a vigilance factor of 0.7, and an iteration  
305 number of 20. The previous ambient aerosol SPAMS dataset (1,400 particles) was used for  
306 the matrix size of the ART-2a is around  $7 \times 10^7$ . The LR-SPAMS data, whose m/z was at  
307 integer level, was generated by summing high resolution SPAMS peaks in each integer m/z  
308 bin. The classification results show that the HR-SPAMS data was grouped to 93 categories  
309 and the top 45 categories accounted for 96 percent of all particles. The particle number of  
310 the first eight categories was 122, 101, 99, 86, 82, 70, 68 and 60 respectively. In contrast,  
311 the LR-SPAMS data was only grouped to 33 categories in total and the top 20 categories  
312 accounted for the 96 percent of all particles. The particle number of the first eight categories  
313 was 170, 118, 107, 107, 106, 92, 90 and 88 respectively. The detailed results can be found  
314 in the Fig.S5-S6. Obviously, ART-2a classification of high resolution SPAMS data  
315 generated more particle categories. This is mainly because HR-SPAMS mass spectra can  
316 differentiate peaks with close m/z, which may be viewed as one peak in LR-SPAMS data.

317

318

319 The ART-2a classification of the HR-SPAMS results (Fig.S6) show that the signal at  
320  $23[\text{Na}^+]$  in Type 2HR was stronger than Type 1HR while the signals at  $26[\text{CN}^-]$  and  
321  $42[\text{CNO}^-]$  were weaker in Type 1 HR. Meanwhile the averaged mass spectra of the Type  
322 2HR showed the presence of  $206[\text{Pb}^+]$ ,  $207[\text{Pb}^+]$  and  $208[\text{Pb}^+]$ , which are known to be  
323 harmful to human health (Das et al., 2018; Peng et al., 2020). Furthermore, particles of  
324 Type 2HR containing abundant secondary inorganic components like  $[\text{NO}_2^-]$ ,  $[\text{NO}_3^-]$  and  
325  $[\text{SO}_4^-]$ , which originated from the aerosol aging processes (Dall'Osto and Harrison, 2012;  
326 Ma et al., 2016). In contrast, these two first particle types were lumped together into Type  
327 1LR in the LR-SPAMS classification results (Fig.S5). Due to the merge of these two  
328 particle types,  $[\text{Pb}^+]$  ions were not significant. Meanwhile, Type 3,4,5HR classification  
329 results contain strong signals at  $26[\text{CN}^-]$ ,  $42[\text{CNO}^-]$ ,  $46[\text{NO}_2^-]$ ,  $62[\text{NO}_3^-]$  and  $97[\text{HSO}_4^-]$ ,  
330 suggesting that these three types were from biomass burning or residential cooking burning.  
331  $[\text{K}^+]$  is also another feature of this type particle emission (Bi et al., 2011; Hudson et al.,  
332 2004). There were obvious relative ion intensity differences at  $26[\text{CN}^-]$ ,  $42[\text{CNO}^-]$ ,  
333  $46[\text{NO}_2^-]$  and  $62[\text{NO}_3^-]$  among these types, which implied that these three particle types

334 might be from different burning sources or experienced different levels of aging (Luo et  
335 al., 2020). While these three particle types were lumped together as Type 2LR. This critical  
336 information which could be potentially used to distinguish particle sources and aging  
337 processes was lost. Additionally, Type 7HR can be assigned as ECOC type, based on its  
338 strong signals at  $[C_x^+]$ ,  $[C_xH_y^+]$  and  $[C_xH_yO_z^+]$ . Particles of this type may come from the  
339 primary emission sources, and the emitted black carbon particles would also form this type  
340 particles after absorbing some low volatile organic compounds in the atmosphere  
341 (Sodeman et al., 2005).  $97[HSO_4^-]$  can be observed to have a weaker signal than  $62[NO_3^-]$   
342 and  $46[NO_2^-]$ , which implied that the secondary reaction of  $SO_2$  as the precursor of  $HSO_4^-$   
343 was not significant in the particle surface for ECOC type particles in this study  
344 (SULLIVAN and PRATHER, 2007). In contrast, the classification results of the LR-  
345 SPAMS were not so clear and generated less particle types. Given HR-SPAMS spectra  
346 have much more detailed chemical information about particles, we would propose that the  
347 ART-2a classification of HR-SPAMS might be more accurate.

348

349

## 350 **5. Conclusion**

351 An automatic linear calibration method had been developed for data analysis of high-  
352 resolution SPAMS data. This technique can significantly improve the m/z accuracy of  
353 SPAMS spectra for atmospheric aerosol samples. The analysis of HR-SPAMS data for  
354 laboratory generated sea spray aerosols shows many details of its chemical compositions.  
355 For example, many organic ions, such as  $C_2H_3^+$  and  $CS^+$ , can be directly determined. The  
356 chemical compositions of ambient aerosols are much more complicated. It is found that,  
357 besides major ions (e.g.  $Na^+$ ,  $K^+$ ,  $Ca^+$ ,  $Fe^+$ ,  $Cl^-$ ,  $CN^-$ ,  $NO_3^-$  and  $HSO_4^-$ ),  $C_xH_y$ ,  $C_xH_yO_z$  and  
358  $CNO^-$  can be identified. With this method, HR-SPAMS can also determine the time series  
359 of organic and inorganic peaks, whose m/z are very close to each other (e.g.  $41K^+$  with the  
360 theoretical m/z value at 40.96182 and  $C_3H_5^+$  with the theoretical m/z value at 41.03913).  
361 Important organic ion peaks, such as tracer peaks for secondary organic matter like  
362  $139[C_2H_3O_5S^-]$  and  $153[C_3H_5O_5S^-]$ , can be identified. More importantly, our ART-2a  
363 classification from HR-SPAMS dataset clearly showed a particle type containing heavy  
364 metals like  $Pb^+$ , which was obviously ignored in the ART-2a classification from the LR-

365 SPAMS dataset. More particle types were generated by the ART-2a classification of HR-  
366 SPAMS data compared to that of LR-SPAMS data, as the original biomass burning particle  
367 type can be divided into three more detailed types based on the different signals of 26[CN<sup>-</sup>],  
368 42[CNO<sup>-</sup>], 46[NO<sub>2</sub><sup>-</sup>] and other organic species like C<sub>x</sub>H<sub>y</sub> and C<sub>x</sub>H<sub>y</sub>O<sub>z</sub>, implying different  
369 aerosol aging processes or burning conditions. Such detailed information may be critical  
370 to study the aging processes and source appointment of atmospheric aerosols. There is a  
371 deficiency of this HR-SPAMS calibration method, which has been showed that some  
372 fraction of particles cannot be calibrated due to the presence of weak signals of the marker  
373 ions. It can be mitigated by applying some additional marker ions. All the automatic linear  
374 calibration method codes specific for HR-SPAMS are open access and can be found at  
375 <https://github.com/zhuxiaoqiang-fdu/zhuxiaoqiang-fdu>. And we proposed the principle of  
376 this calibration method can be adopted in other aerosol mass spectrometers.

377

378

### 379 **Author Contribution**

380 Y.X and X.W. supervised this study. X.W. and S.Z. designed the calibration and data  
381 analysis methods. S. Wang. and S.Z. performance the sea spray aerosol and ambient aerosol  
382 experiment. S.Z. wrote the open source code for calibration and data analysis of the single  
383 particle mass spectra and made the GUI program with suggestions from X.W. and X.Y..  
384 X.W. and S.Z. prepared the manuscript with contributions from all co-authors.

385

### 386 **Acknowledgments**

387 This work was partially supported by the National Natural Science Foundation of China  
388 (Nos. 41827804, 41775150, 21906024, 91544224) and Shanghai Natural Science  
389 Foundation (No. 19ZR1404000). The authors thank Hexin Analytical Instrument Co., Ltd.,  
390 China for providing HR-SPAMS.

391

### 392 **Competing interests**

393 The authors declare that they have no conflict of interest.

394

395



396 **Reference**

- 397 Ackerman, A. S., Kirkpatrick, M. P., Stevens, D. E., and Toon, O. B.: The impact of humidity above  
398 stratiform clouds on indirect aerosol climate forcing, *Nature*, 432, 1014-1017, 2004.
- 399 Bertram, T. H., Cochran, R. E., Grassian, V. H., and Stone, E. A.: Sea spray aerosol chemical composition:  
400 elemental and molecular mimics for laboratory studies of heterogeneous and multiphase reactions,  
401 *Chemical Society Reviews*, 2018. 10.1039.C1037CS00008A, 2018.
- 402 Bi, X., Zhang, G., Li, L., Wang, X., Li, M., Sheng, G., Fu, J., and Zhou, Z.: Mixing state of biomass burning  
403 particles by single particle aerosol mass spectrometer in the urban area of PRD, China, *Atmospheric  
404 Environment*, 45, 3447-3453, 2011.
- 405 Chudinov, A., Li, L., Zhou, Z., Huang, Z., Gao, W., Yu, J., Nikiforov, S., Pikhtev, A., Bukharina, A., and  
406 Kozlovskiy, V.: Improvement of peaks identification and dynamic range for bi-polar Single Particle Mass  
407 Spectrometer, *International Journal of Mass Spectrometry*, 436, 7-17, 2019.
- 408 Collins, D. B., Zhao, D. F., Ruppel, M. J., Laskina, O., Grandquist, J. R., Modini, R. L., Stokes, M. D., Russell,  
409 L. M., Bertram, T. H., and Grassian, V. H.: Direct aerosol chemical composition measurements to evaluate  
410 the physicochemical differences between controlled sea spray aerosol generation schemes,  
411 *Atmospheric Measurement Techniques Discussions*, 7, 6457-6499, 2014.
- 412 Dall'Osto and Harrison, M.: Urban organic aerosols measured by single particle mass spectrometry in  
413 the megacity of London, *ATMOSPHERIC CHEMISTRY and PHYSICS*, 12, 2012.
- 414 Das, R., Bin Mohamed Mohtar, A. T., Rakshit, D., Shome, D., and Wang, X.: Sources of atmospheric lead  
415 (Pb) in and around an Indian megacity, *Atmospheric Environment*, 193, 57-65, 2018.
- 416 Hudson, P. K., Murphy, D. M., Cziczo, D. J., Thomson, D. S., Gouw, J. A. D., Warneke, C., Holloway, J., Jost, H.  
417 J., and Hübler, G.: Biomass - burning particle measurements: Characteristic composition and chemical  
418 processing, *Journal of Geophysical Research Atmospheres*, 109, 2004.
- 419 Li, L., Liu, L., Xu, L., Li, M., Li, X., Gao, W., Huang, Z., and Cheng, P.: Improvement in the Mass Resolution  
420 of Single Particle Mass Spectrometry Using Delayed Ion Extraction, *Journal of the American Society for  
421 Mass Spectrometry*, 29, 2105-2109, 2018.
- 422 Luo, J., Zhang, J., Huang, X., Liu, Q., Luo, B., Zhang, W., Rao, Z., and Yu, Y.: Characteristics, evolution, and  
423 regional differences of biomass burning particles in the Sichuan Basin, China, *Journal of Environmental  
424 Sciences*, 89, 35-46, 2020.
- 425 Ma, L., Li, M., Huang, Z., Li, L., Gao, W., Nian, H., Zou, L., Fu, Z., Gao, J., Chai, F., and Zhou, Z.: Real time  
426 analysis of lead-containing atmospheric particles in Beijing during springtime by single particle  
427 aerosol mass spectrometry, *Chemosphere*, 154, 454-462, 2016.
- 428 Manuel, D. O., Harrison, R. M., Beddows, D. C. S., Freney, E. J., Heal, M. R., and Donovan, R. J.: Single-  
429 particle detection efficiencies of aerosol time-of-flight mass spectrometry during the North Atlantic  
430 marine boundary layer experiment, *Environmental Science Technology*, 40, 5029-5035, 2006.
- 431 Moffet, R. C. and Prather, K. A.: In-situ measurements of the mixing state and optical properties of soot  
432 with implications for radiative forcing estimates, *Proceedings of the National Academy of Sciences of  
433 the United States of America*, 106, 11872-11877, 2009.
- 434 Murphy, D. M.: The design of single particle laser mass spectrometers, *Mass Spectrometry Reviews*, 26,  
435 150-165, 2010.

436 Nash, D. G., Baer, T., and Johnston, M. V.: Aerosol mass spectrometry: An introductory review,  
437 International Journal of Mass Spectrometry, 258, 2-12, 2006.

438 Peng, M., Zhao, C., Ma, H., Yang, Z., Yang, K., Liu, F., Li, K., Yang, Z., Tang, S., Guo, F., Liu, X., and Cheng, H.:  
439 Heavy metal and Pb isotopic compositions of soil and maize from a major agricultural area in Northeast  
440 China: Contamination assessment and source apportionment, Journal of Geochemical Exploration, 208,  
441 106403, 2020.

442 Pratt, K. A. and Prather, K. A.: Mass spectrometry of atmospheric aerosols-Recent developments and  
443 applications. Part II: On-line mass spectrometry techniques, Mass Spectrometry Reviews, 31, 17-48,  
444 2012.

445 Qin, X., Bhave, P. V., and Prather, K. A.: Comparison of Two Methods for Obtaining Quantitative Mass  
446 Concentrations from Aerosol Time-of-Flight Mass Spectrometry Measurements, Analytical Chemistry,  
447 78, 6169-6178, 2006.

448 Reinard, M. S., Adou, K., Martini, J. M., and Johnston, M. V.: Source characterization and identification by  
449 real-time single particle mass spectrometry, Atmospheric Environment, 41, 9397-9409, 2007.

450 Sodeman, D. A., Toner, S. M., and Prather, K. A.: Determination of Single Particle Mass Spectral Signatures  
451 from Light-Duty Vehicle Emissions, Environmental Science & Technology, 39, 4569-4580, 2005.

452 Song, X.-H., Hopke, P. K., Fergenson, D. P., and Prather, K. A.: Classification of Single Particles Analyzed  
453 by ATOFMS Using an Artificial Neural Network, ART-2A, Analytical Chemistry, 71, 860-865, 1999.

454 SULLIVAN, R. C. and PRATHER, K. A.: Investigations of the Diurnal Cycle and Mixing State of Oxalic Acid  
455 in Individual Particles in Asian Aerosol Outflow, Environmental Science & Technology, 41, p.8062-8069,  
456 2007.

457 Sullivan, R. C. and Prather, K. A.: Recent advances in our understanding of atmospheric chemistry and  
458 climate made possible by on-line aerosol analysis instrumentation, Analytical Chemistry, 77, 3861-  
459 3885, 2005.

460 Surratt, J. D., Chan, A. W. H., Eddingsaas, N. C., Chan, M. N., Loza, C. L., Kwan, A. J., Hersey, S. P., Flagan, R.  
461 C., Wennberg, P. O., and Seinfeld, J. H.: Reactive intermediates revealed in secondary organic aerosol  
462 formation from isoprene, Proceedings of the National Academy of Sciences of the United States of  
463 America, 107, p.6640-6645, 2010.

464 Surratt, J. D., Kroll, J. H., Kleindienst, T. E., Edney, E. O., Claeys, M., Sorooshian, A., Ng, N. L., Offenberg, J.  
465 H., Lewandowski, M., and Jaoui, M.: Evidence for organosulfates in secondary organic aerosol,  
466 Environmental Science & Technology, 41, p. 517-527, 2007.

467 Tsunogai, S., Saito, O., Yamada, K., and Nakaya, S.: Chemical composition of oceanic aerosol, Journal of  
468 Geophysical Research, 77, 5283-5292, 1972.

469 Wang, H., An, J., Shen, L., Zhu, B., Xia, L., Duan, Q., and Zou, J.: Mixing state of ambient aerosols in Nanjing  
470 city by single particle mass spectrometry, Atmospheric Environment, 132, 123-132, 2016.

471 Wang, H., Shen, L., Yin, Y., Chen, K., Chen, J., and Wang, Y.: Characteristics and mixing state of aerosol at  
472 the summit of Mount Tai (1534 m) in Central East China: First measurements with SPAMS,  
473 Atmospheric Environment, 213, 273-284, 2019.

474 Wenzel, R. J., Liu, D. Y., Edgerton, E. S., and Prather, K. A.: Aerosol time - of - flight mass spectrometry  
475 during the Atlanta Supersite Experiment: 2. Scaling procedures, Journal of Geophysical Research:

476 Atmospheres, 2003. 2003.

477 Zelenyuk, A. and Imre, D.: Beyond single particle mass spectrometry: multidimensional  
478 characterisation of individual aerosol particles, *International Reviews in Physical Chemistry*, 28, 309-  
479 358, 2009.

480 Zhang, G., Bi, X., Chan, L. Y., Wang, X., Sheng, G., and Fu, J.: Size-segregated chemical characteristics of  
481 aerosol during haze in an urban area of the Pearl River Delta region, China, *Urban Climate*, 4, 74-84,  
482 2013.

483 Zhang, R. J. and Kin-Fai, H. O.: The Role of Aerosol in Climate Change, the Environment, and Human  
484 Health, *Atmospheric Oceanic Science Letters*, 5, 156-161, 2012.  
485

486

487

488

489

490

491 **Figure Captions**

492

493 **Figure 1.** The GUI program for HR-SPAMS calibration

494 **Figure 2.** Linear calibration with reference ion peaks

495 **Figure 3.** Probability distributions of the marker peak locations before and after Automatic  
496 Linear Calibration (AL-Cal) for (a) sea spray aerosol and (b) ambient aerosol

497 **Figure 4.** Averaged positive and negative mass spectra of sea spray aerosols

498 **Figure 5.** Averaged positive and negative mass spectra of ambient aerosols

499 **Figure 6.** Time series of peak intensities at  $m/z$  40.95 and  $m/z$  41.01

500

501 Table 1. Possible peak assignments for the m/z of reference ions for sea spray aerosol and  
 502 ambient aerosol

Unit resolution	mass m/z	Possible species (Sea spray aerosol)	Unit resolution	mass m/z	Possible species (Ambient aerosol)
+24		Mg <sup>+</sup> C <sub>2</sub> <sup>+</sup>	+39		K <sup>+</sup> C <sub>3</sub> H <sub>3</sub> <sup>+</sup>
+39		K <sup>+</sup> C <sub>3</sub> H <sub>3</sub> <sup>+</sup>	+56		Fe <sup>+</sup> Si <sub>2</sub> <sup>+</sup> CaO <sup>+</sup> KOH <sup>+</sup>
+81		Na <sub>2</sub> Cl <sup>+</sup> Br <sup>+</sup> C <sub>6</sub> H <sub>9</sub> <sup>+</sup>	-26		CN <sup>-</sup> BO <sup>-</sup> C <sub>2</sub> H <sub>2</sub> <sup>-</sup>
+113		K <sub>2</sub> Cl <sup>+</sup> C <sub>9</sub> H <sub>5</sub> <sup>+</sup>	-62		NO <sub>3</sub> <sup>-</sup> C <sub>5</sub> H <sub>2</sub> <sup>-</sup>
+115		K <sub>2</sub> Cl <sup>+</sup> C <sub>9</sub> H <sub>7</sub> <sup>+</sup>	-96		SO <sub>4</sub> <sup>-</sup> BrOH <sup>-</sup>
-26		CN <sup>-</sup> BO <sup>-</sup> C <sub>2</sub> H <sub>2</sub> <sup>-</sup>	-97		HSO <sub>4</sub> <sup>-</sup> C <sub>8</sub> H <sup>-</sup> BrO <sup>-</sup> NaCl <sub>2</sub> <sup>-</sup> H <sub>2</sub> PO <sub>4</sub> <sup>-</sup>
-37		Cl <sup>-</sup> C <sub>3</sub> H <sup>-</sup>			
-42		BO <sub>2</sub> <sup>-</sup> CNO <sup>-</sup>			
-129		MgCl <sub>3</sub> <sup>-</sup> C <sub>10</sub> H <sub>9</sub> <sup>-</sup> (C <sub>3</sub> H <sub>7</sub> ) <sub>2</sub> C <sub>2</sub> H <sub>5</sub> <sup>-</sup> CaCl <sub>2</sub> OH <sup>-</sup>			
-131		MgCl <sub>3</sub> <sup>-</sup>			

503

504

505

506

507

508

509

510 Table 2. Peak identification of important chemical species in sea spray aerosols. The first  
 511 column is the measured m/z for peaks. The second and third columns shows the theoretical  
 512 m/z bin value and theoretical m/z value of most possible species for each peak

Measurement m/z(positive)	Possible species (theoretical m/z bin value)	Possible species (theoretical m/z value)	Measurement m/z(negative)	Possible species (theoretical m/z bin value)	Possible species (theoretical m/z value)
22.993	Na <sup>+</sup> (22.993)	Na <sup>+</sup> (22.98977)	15.0344	CH <sub>3</sub> <sup>-</sup> (15.0216)	CH <sub>3</sub> <sup>-</sup> (15.02348)
23.9829	Mg <sup>+</sup> (23.9829)	Mg <sup>+</sup> (23.98505)	34.9641	Cl <sup>-</sup> (34.9641)	Cl <sup>-</sup> (34.96885)
27.0267	C <sub>2</sub> H <sub>3</sub> <sup>+</sup> (27.0267)	C <sub>2</sub> H <sub>3</sub> <sup>+</sup> (27.02348)	41.9864	CNO <sup>-</sup> (41.9971)	CNO <sup>-</sup> (41.99799)
38.9672	K <sup>+</sup> (38.9672)	K <sup>+</sup> (38.96371)	25.0163	C <sub>2</sub> H <sup>-</sup> (25.0081)	C <sub>2</sub> H <sup>-</sup> (25.00783)
39.9711	Ca <sup>+</sup> (39.9607)	Ca <sup>+</sup> (39.96259)	38.0024	C <sub>3</sub> H <sub>2</sub> <sup>-</sup> (38.0126)	C <sub>3</sub> H <sub>2</sub> <sup>-</sup> (38.01565)
43.9614	CS <sup>+</sup> (43.9723)	CS <sup>+</sup> (43.9721)	44.9883	HCO <sub>2</sub> <sup>-</sup> (44.9994)	HCO <sub>2</sub> <sup>-</sup> (44.99767)
45.983	Na <sub>2</sub> <sup>+</sup> (45.983)	Na <sub>2</sub> <sup>+</sup> (45.97954)	49.002	C <sub>4</sub> H <sup>-</sup> (49.0135)	C <sub>4</sub> H <sup>-</sup> (49.00783)
59.9569	SiO <sub>2</sub> <sup>+</sup> (59.9696)	SiO <sub>2</sub> <sup>+</sup> (59.96677)	57.9574	NaCl <sup>-</sup> (57.9574)	NaCl <sup>-</sup> (57.95865)
71.9872	C <sub>6</sub> <sup>+</sup> (72.0012)	C <sub>6</sub> <sup>+</sup> (72)			
80.9438	Na <sub>2</sub> Cl <sup>+</sup> (80.9438)	Na <sub>2</sub> Cl <sup>+</sup> (80.94839)	63.9574	SO <sub>2</sub> <sup>-</sup> (63.9574)	SO <sub>2</sub> <sup>-</sup> (63.96191)
112.898	K <sub>2</sub> Cl <sup>+</sup> (112.898)	K <sub>2</sub> Cl <sup>+</sup> (112.89627)	75.9498	SiO <sub>3</sub> <sup>-</sup> (75.9642)	SiO <sub>3</sub> <sup>-</sup> (75.96196)
138.89	Na <sub>3</sub> Cl <sub>2</sub> <sup>+</sup> (138.907)	Na <sub>3</sub> Cl <sub>2</sub> <sup>+</sup> (138.90702)			
140.897	Na <sub>3</sub> Cl <sub>2</sub> <sup>+</sup> (140.897)	Na <sub>3</sub> Cl <sub>2</sub> <sup>+</sup> (140.90407)	79.9547	SO <sub>3</sub> <sup>-</sup> (79.9547)	SO <sub>3</sub> <sup>-</sup> (79.95683)
			80.9015	Br <sup>-</sup> (80.9164)	Br <sup>-</sup> (80.91629)
			85.9484	NaPO <sub>2</sub> <sup>-</sup> (85.9484)	NaPO <sub>2</sub> <sup>-</sup> (85.95337)
			99.9499	CaCO <sub>3</sub> <sup>-</sup> (99.9499)	CaCO <sub>3</sub> <sup>-</sup> (99.94735)
			109.917	CaCl <sub>2</sub> <sup>-</sup> (109.9)	CaCl <sub>2</sub> <sup>-</sup> (109.9003)
			128.901	MgCl <sub>3</sub> <sup>-</sup> (128.883)	MgCl <sub>3</sub> <sup>-</sup> (128.89161)

513

514

515

516

517

518

519

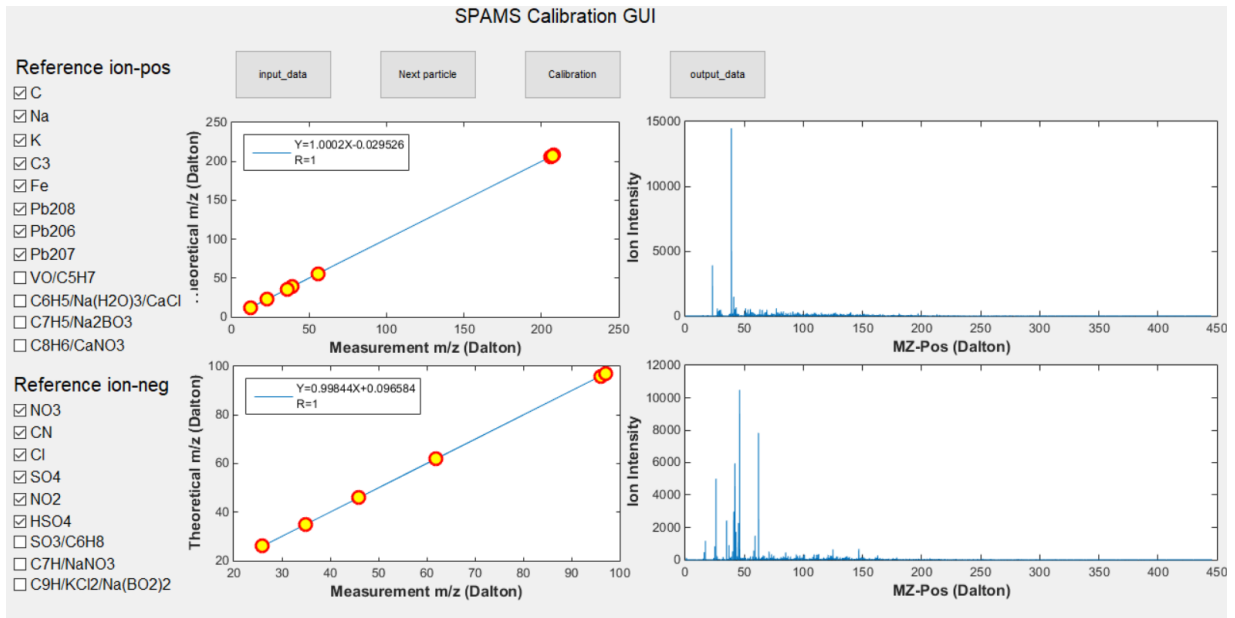
520 Table 3. Peak identification of important chemical species in ambient aerosols. The first  
 521 column is the measured m/z for each peak. The second and third columns shows the  
 522 theoretical m/z bin value and theoretical m/z value of most possible specie for each peak

Measurement m/z(positive)	Possible species(theoretical m/z bin value)	Possible species(theoretical m/z value)	Measurement m/z(negative)	Possible species(theoretical m/z bin value)	Possible species(theoretical m/z value)
22.993	Na <sup>+</sup> (22.993)	Na <sup>+</sup> (22.98977)	15.0408	CH <sub>3</sub> <sup>-</sup> (15.0216)	CH <sub>3</sub> <sup>-</sup> (15.02348)
23.9991	C <sub>2</sub> <sup>+</sup> (23.9991)	C <sub>2</sub> <sup>+</sup> (24)	16.0091	O <sup>-</sup> (15.9959)	O <sup>-</sup> (15.99492)
25.002	C <sub>2</sub> H <sup>+</sup> (25.0103)	C <sub>2</sub> H <sup>+</sup> (25.00783)	17.0145	OH <sup>-</sup> (17.0009)	OH <sup>-</sup> (17.00275)
26.0087	C <sub>2</sub> H <sub>2</sub> <sup>+</sup> (26.0171)	C <sub>2</sub> H <sub>2</sub> <sup>+</sup> (26.01565)	26.0078	CN <sup>-</sup> (25.9994)	CN <sup>-</sup> (26.00307)
30.0171	NO <sup>+</sup> (29.999)	NO <sup>+</sup> (29.99799)	31.987	O <sub>2</sub> <sup>-</sup> (31.987)	O <sub>2</sub> <sup>-</sup> (31.98984)
35.9925	C <sub>3</sub> <sup>+</sup> (36.0023)	C <sub>3</sub> <sup>+</sup> (36)	34.9641	Cl <sup>-</sup> (34.9641)	Cl <sup>-</sup> (34.96885)
36.9976	C <sub>3</sub> H <sup>+</sup> (37.0076)	C <sub>3</sub> H <sup>+</sup> (37.00783)	41.9971	CNO <sup>-</sup> (41.9971)	CNO <sup>-</sup> (41.99799)
38.0065	C <sub>3</sub> H <sub>2</sub> <sup>+</sup> (38.0166)	C <sub>3</sub> H <sub>2</sub> <sup>+</sup> (38.01565)	45.9897	NO <sub>2</sub> <sup>-</sup> (45.9897)	NO <sub>2</sub> <sup>-</sup> (45.99291)
38.9672	K <sup>+</sup> (38.9672)	K <sup>+</sup> (38.96371)	47.9911	C <sub>4</sub> <sup>-</sup> (47.993)	C <sub>4</sub> <sup>-</sup> (48)
47.993	C <sub>4</sub> <sup>+</sup> (47.993)	C <sub>4</sub> <sup>+</sup> (48)	61.9808	NO <sub>3</sub> <sup>-</sup> (61.9938)	NO <sub>3</sub> <sup>-</sup> (61.98783)
48.9911	C <sub>4</sub> H <sup>+</sup> (49.0026)	C <sub>4</sub> H <sup>+</sup> (49.00783)	71.0014	C <sub>3</sub> H <sub>3</sub> O <sub>2</sub> <sup>-</sup> (71.0153)	C <sub>3</sub> H <sub>3</sub> O <sub>2</sub> <sup>-</sup> (71.01332)
49.9994	C <sub>4</sub> H <sub>2</sub> <sup>+</sup> (50.0111)	C <sub>4</sub> H <sub>2</sub> <sup>+</sup> (50.01565)	78.9548	PO <sub>3</sub> <sup>-</sup> (78.9548)	PO <sub>3</sub> <sup>-</sup> (78.95852)
55.9443	Fe <sup>+</sup> (55.932)	Fe <sup>+</sup> (55.93494)	79.94	SO <sub>3</sub> <sup>-</sup> (79.9547)	SO <sub>3</sub> <sup>-</sup> (79.95683)
59.9951	C <sub>5</sub> <sup>+</sup> (59.9951)	C <sub>5</sub> <sup>+</sup> (60)	80.946	HSO <sub>3</sub> <sup>-</sup> (80.9609)	HSO <sub>3</sub> <sup>-</sup> (80.96466)
60.9946	C <sub>5</sub> H <sup>+</sup> (61.0074)	C <sub>5</sub> H <sup>+</sup> (61.00783)	95.9825	SO <sub>4</sub> <sup>-</sup> (95.9502)	SO <sub>4</sub> <sup>-</sup> (95.95175)
62.0023	C <sub>5</sub> H <sub>2</sub> <sup>+</sup> (62.0152)	C <sub>5</sub> H <sub>2</sub> <sup>+</sup> (62.01565)	96.9546	HSO <sub>4</sub> <sup>-</sup> (96.9546)	HSO <sub>4</sub> <sup>-</sup> (96.95958)
72.0012	C <sub>6</sub> <sup>+</sup> (72.0012)	C <sub>6</sub> <sup>+</sup> (72)	121.01	C <sub>10</sub> H <sup>-</sup> (121.01)	C <sub>10</sub> H <sup>-</sup> (121.00783)
84.0108	C <sub>7</sub> <sup>+</sup> (83.9957)	C <sub>7</sub> <sup>+</sup> (84)	122.01	C <sub>10</sub> H <sub>2</sub> <sup>-</sup> (122.01)	C <sub>10</sub> H <sub>2</sub> <sup>-</sup> (122.01565)
207.976	Pb <sup>+</sup> (207.967)	Pb <sup>+</sup> (207.97664)	134.008	C <sub>11</sub> H <sub>2</sub> <sup>-</sup> (134.008)	C <sub>11</sub> H <sub>2</sub> <sup>-</sup> (134.01565)

523

524

525



526

527

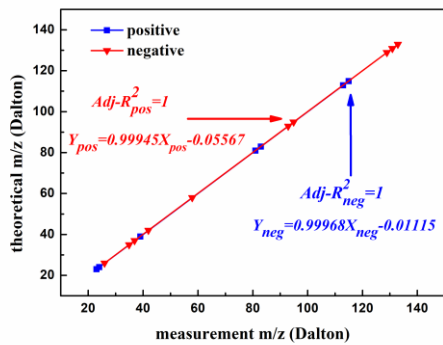
528

529

Figure 1. The GUI program for HR-SPAMS calibration

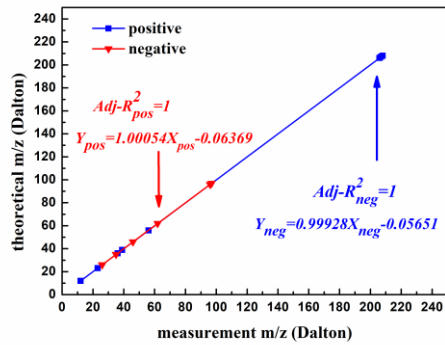


530



531

(a) sea spray aerosol



532

(b) ambient aerosol

533

534

Figure 2. Linear calibration with reference ion peaks

535

536

537

538

539

540

541

542

543

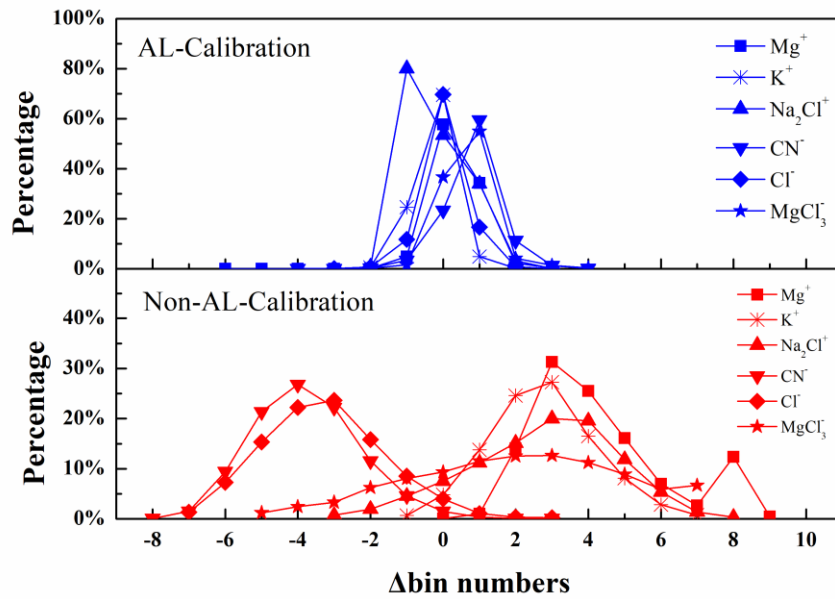
544

545

546

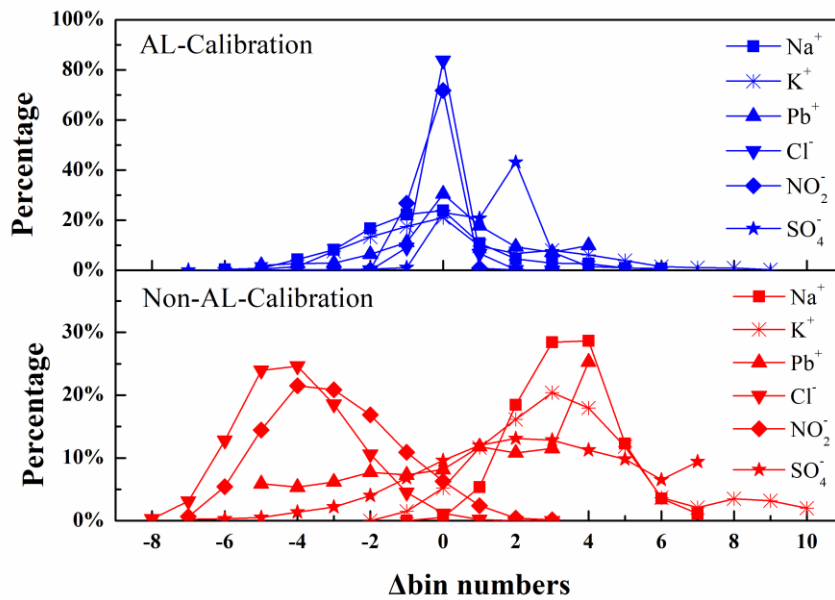
547

548 a.



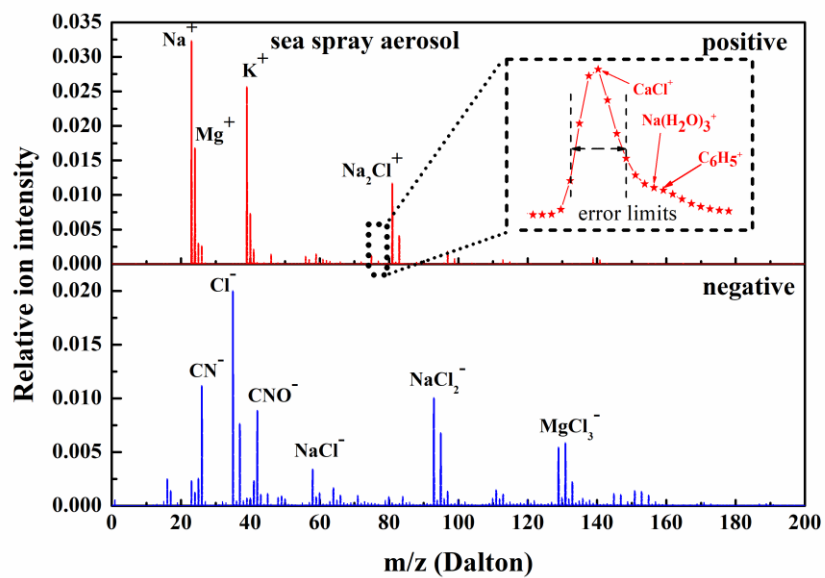
549

550 b.



551

552 Figure 3. Probability distributions of the marker peak locations before and after Automatic  
553 Linear Calibration (AL-Cal) for (a) sea spray aerosol and (b) ambient aerosol

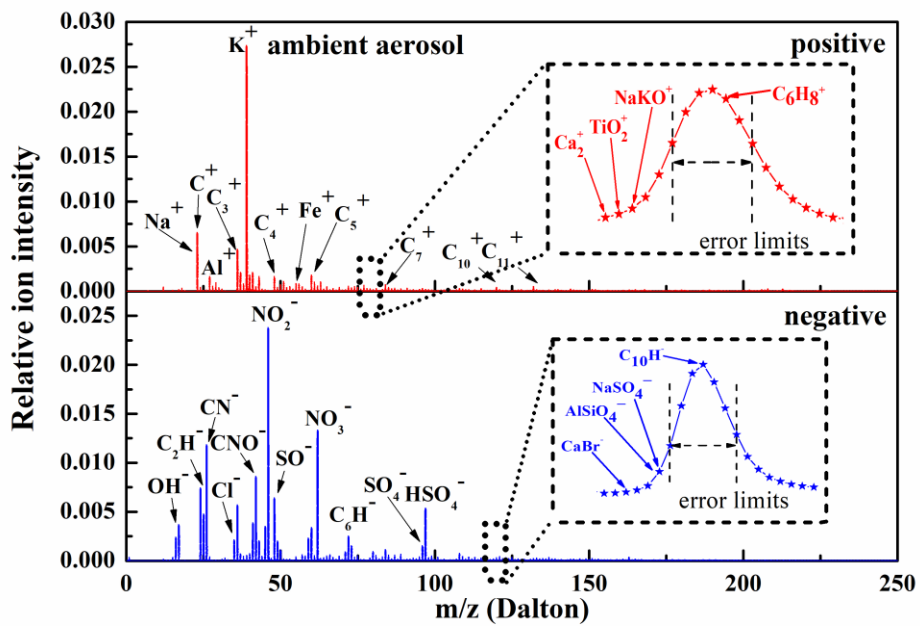


555

556

Figure 4. Averaged positive and negative mass spectra of sea spray aerosols

557



558

559

Figure 5. Averaged positive and negative mass spectra of ambient aerosols

560

561

562

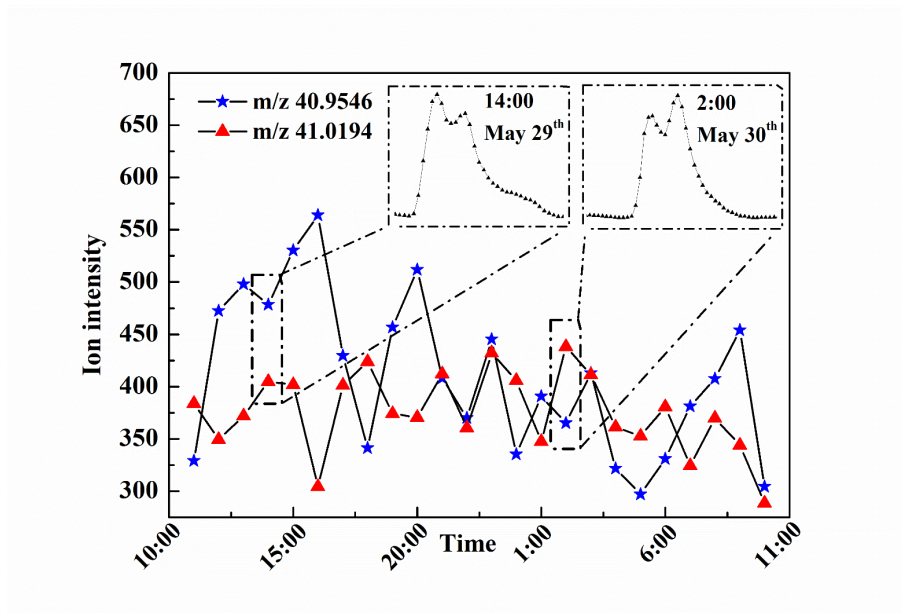


Figure 6. Time series of peak intensities at m/z 40.95 and m/z 41.01

564

565

566

567